

# Capturing points with a rotating polygon (and a 3D extension)

Carlos Alegría-Galicia <sup>1</sup>, David Orden <sup>2</sup>, Leonidas Palios <sup>3</sup>, Carlos Seara <sup>4</sup>, and Jorge Urrutia <sup>5</sup>

<sup>1</sup> Posgrado en Ciencia e Ingeniería de la Computación, Universidad Nacional Autónoma de México. [calegria@uxmcc2.iimas.unam.mx](mailto:calegria@uxmcc2.iimas.unam.mx)

<sup>2</sup>Departamento de Física y Matemáticas, Universidad de Alcalá, Spain. [david.orden@uah.es](mailto:david.orden@uah.es)

<sup>3</sup>Department of Computer Science and Engineering, University of Ioannina, Greece. [palios@cs.uoi.gr](mailto:palios@cs.uoi.gr)

<sup>4</sup>Departament de Matemàtiques, Universitat Politècnica de Catalunya, Spain. [carlos.seara@upc.edu](mailto:carlos.seara@upc.edu)

<sup>5</sup>Instituto de Matemáticas, Universidad Nacional Autónoma de México. [urrutia@matem.unam.mx](mailto:urrutia@matem.unam.mx)

## Abstract

We study the problem of rotating a simple polygon to contain the maximum number of elements from a given point set in the plane. We consider variations of this problem where the rotation center is a given point or lies on a line segment, a line, or a polygonal chain. We also solve an extension to 3D where we rotate a polyhedron around a given point to contain the maximum number of elements from a set of points in the space.

**Keywords:** Points covering, rotation, geometric optimization, polygon, polyhedron.

## 1 Introduction

Given a simple polygon  $P$  on the plane, the *Polygon Placement Problem* consists in finding a function  $\tau$ , usually consisting of the composition of a rotation and a translation, such that  $\tau(P)$  satisfies some geometric constraints. In the literature,  $\tau(P)$  is known as a *placement* of  $P$ . The oldest problem of this family who, given two polygons  $P$  and  $Q$ , explored the problem of finding, if it exists, a placement of  $P$  that contains  $Q$ . The most recent contribution to these problems, in 2014, can be found in [2] (see Section 1.4

there for a summary of previous work). Among other results, for a point set  $S$  and a simple polygon  $P$ , they show how to compute a placement of  $P$  that contains as many points of  $S$  as possible. If  $n$  and  $m$  are the sizes of  $S$  and  $P$  respectively, their algorithm runs in  $O(n^3 m^3 \log(nm))$  time and  $O(nm)$  space.

Although translation-only problems have also been considered [1, 4], surprisingly enough there are no previous results with  $\tau$  being only a rotation. It is important to note that existing results with  $\tau$  being a composition of a rotation, a translation, and even a scaling, cannot be adapted to solve the rotation-only problem considered here: All those previous results reduce the search space complexity by considering only placements where a constant number of points from  $S$  lie on the boundary of  $P$  (see for example references [2] and [6] for algorithms based respectively, on two-point and one-point placements). Rotation-only adaptations of these results would not allow the rotation center to be fixed or restricted to lie on a given curve and therefore, cannot be applied to the problems we deal with in this paper. This is why the following *Maximum Cover under Rotation (MCR)* problems are considered in this paper:

**Problem 1** (Fixed MCR). *Given a point  $r$ , a polygon  $P$ , and a point set  $S$  in the plane, compute an angle  $\theta \in [0, 2\pi)$  such that, after clockwise rotating  $P$  around  $r$  by  $\theta$ , the number of points of  $S$  contained in  $P$  is maximized.*

**Problem 2** (Segment-restricted MCR). *Given a line segment  $\ell$ , a polygon  $P$ , and a point set  $S$  in the plane, find a point  $r$  on  $\ell$  and an angle  $\theta \in [0, 2\pi)$  such that, after a clockwise rotating of  $P$  around  $r$  by  $\theta$ , the number of points of  $S$  contained in  $P$  is maximized.*

In addition, we complete the scene opening a path towards the study of these problems in 3D, by presenting a three-dimensional version of Problem 1:

**Problem 3** (3D Fixed MCR). *Given a point  $r$ , a polyhedron  $P$ , and a point set  $S$  in  $\mathbb{R}^3$ , compute the azimuth and altitude  $(\theta, \varphi) \in [0, 2\pi] \times [-\pi, \pi]$  giving the direction in the unit sphere such that, after rotating a polyhedron  $P$  by taking the  $z$ -axis to that direction, the number of points of  $S$  contained in  $P$  is maximized.*

Applications of polygon placement problems include global localization of mobile robots, pattern matching, and geometric tolerance; see the references in [2]. Rotation-only problems arise, e.g., in robot localization using a rotating camera [8], with applications to quality control of objects manufactured around an axis [10].

We first show that Problem 1 is 3SUM-hard, i.e., solving it in sub-quadratic time would imply an affirmative answer to the open question

of whether a subquadratic time algorithm for 3SUM exists, which is unlikely [7]. Then, we present two algorithms to solve Problem 1: The first one requires  $O(nm \log(nm))$  time and  $O(nm)$  space, for  $n$  and  $m$  being the sizes of  $S$  and  $P$ , respectively. The second one takes  $O((n+k) \log n + m \log m)$  time and  $O(n+m+k)$  space, for  $k$  in  $O(nm)$  being the number of certain events. We also describe an algorithm that solves Problem 2 in  $O(n^2 m^2 \log(nm))$  time and  $O(n^2 m^2)$  space. This algorithm can be easily extended to solve variations of Problem 2 where  $r$  lies on a line or a polygonal chain. Furthermore, our techniques for Problem 1 can be extended to 3D to solve Problem 3 within the same time and space complexities as Problem 2.

## 2 Fixed MCR (Problem 1)

Given a point  $r$  on the plane and a point  $p \in S$ , let  $C_p(r)$  be the circle with center  $r$  and radius  $|\overline{rp}|$ . If we rotate  $S$  in the counterclockwise direction around  $r$ ,  $C_p(r)$  is the curve described by  $p$  during a  $2\pi$  rotation of  $S$  around  $r$ . The endpoints of the circular arcs resulting from intersecting  $P$  and  $C_p(r)$  determine the rotation angles where  $p$  enters (*in-event*) and leaves (*out-event*) the polygon  $P$ . In the worst case, the number of such events per element of  $S$  is  $O(m)$ , see Figure 1. If we consider all the points in  $S$  we could get  $O(nm)$  events.

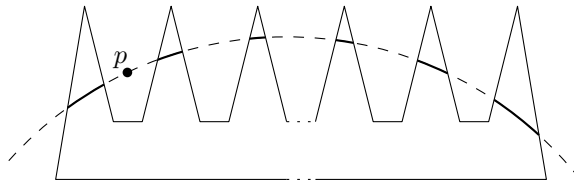


Figure 1: A comb-shaped simple polygon can generate  $\Omega(m)$  in- and out-events per point in  $S$ .

### 2.1 A 3SUM-hard reduction

We show next that Problem 1 is 3SUM-hard, by a reduction from the *Segments Containing Points Problem* that was proved to be 3SUM-hard in [3]: Given a set  $A$  of  $n$  real numbers and a set  $B$  of  $m = O(n)$  pairwise-disjoint intervals on the real line, is there a real number  $u$  such that  $A + u \subseteq B$ ?

**Theorem 4.** *The Fixed MCR problem is 3SUM-hard.*

*Proof.* Let  $I$  be an interval of the real line that contains the set  $A$  of points, and the set  $B$  of intervals of an instance of the Segments Containing Points Problem. Wrap  $I$  on a circle  $C$  whose perimeter has length at least twice

the length of  $I$ . This effectively maps the points in  $A$  and the intervals in  $B$  into a set  $A'$  of points and a set  $B'$  of intervals on  $C$ .

Clearly, finding a translation (if it exists) of the elements of  $A$  such that  $A + u \subseteq B$ , is equivalent to finding a rotation of the set of points  $A'$  around the center of  $C$  such that all of the elements of  $A'$  are mapped to points contained in the intervals of  $B'$ . To finish our reduction, construct a

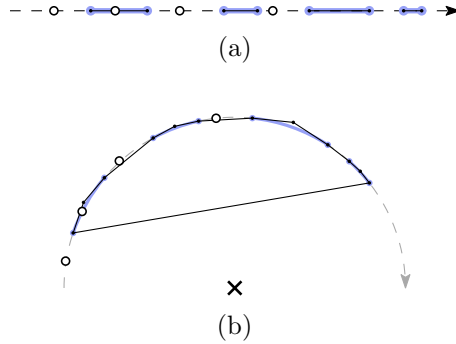


Figure 2: Wrapping  $I$  from (a) the real line to (b) a circle  $C$ . Intervals forming  $B$  and  $B'$  are highlighted with blue. Elements of  $A$  and  $A'$  are represented by white points. Additional vertices forming the polygon are the intersection points between the tangents to  $C$  at the endpoints of each interval in  $B'$ .

polygon as shown in Figure 2. □

## 2.2 An $O(nm \log(nm))$ algorithm

Here we present an  $O(nm \log(nm))$  algorithm for Problem 1 (note that, by Theorem 4, this complexity is close to be optimal):

1. **Intersect rotation circles.** Given a fixed point  $r$ , compute the intersection points of  $C_{p_j}(r)$  and  $P$ , for all  $p_j \in S$ . Each of these points determines an angle of rotation of  $p_j$  around  $r$  when  $p_j$  enters or leaves  $P$ , see Figure 3. These angles, in turn, determine a set of intervals  $\mathcal{I} = \{I_{j,1}, \dots, I_{j,m_j}\}$  whose endpoints correspond to the rotation angles in which  $p_j$  enters or leaves  $P$  and, hence, specify the rotation angles on the unit circle for which  $p_j$  belongs to  $P$ , see again Figure 3. Let  $\mathcal{I} = \mathcal{I}_1 \cup \dots \cup \mathcal{I}_n$ . The set of endpoints of the intervals in  $\mathcal{I}$  can be sorted in  $O(mn \log(mn))$  time.
2. **Compute the angle of maximum coverage.** Using standard techniques, we can now perform a sweep on the set  $\mathcal{I} = \mathcal{I}_1 \cup \dots \cup \mathcal{I}_n$  as depicted in Figure 4. During the sweeping process, we maintain the number of points of  $S$  lying in  $P$ . If an in-event or an out-event occurs, that number is increased or decreased by one, respectively. At the end

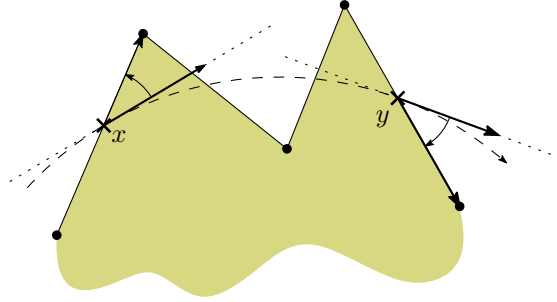


Figure 3: An in-event at  $x$  (left turn), and an out-event at  $y$  (right turn).

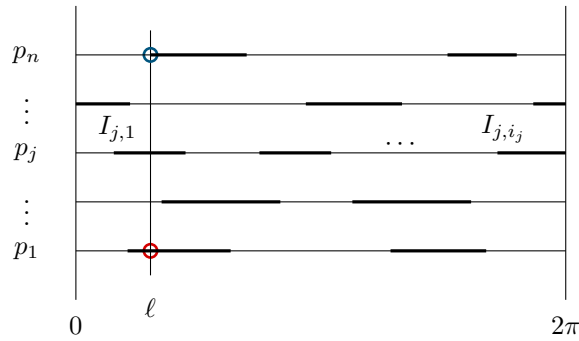


Figure 4: The events sequence and the sweeping line at angle  $\theta$ . Highlighted with a red circle, the intersection of line  $\ell$  with an interval corresponding to  $p_1$  (where  $p_1$  is inside  $P$ ). Highlighted with a blue circle, the intersection of line  $\ell$  with one of the endpoints of an interval corresponding to  $p_n$  (an in-event).

of the sweeping process, we report the angular interval(s) where the number is maximized.

Since the complexity of our algorithm is dominated by Step 1, which takes  $O(nm \log(nm))$  time, we conclude the following result.

**Theorem 5.** *The Fixed MCR problem can be solved in  $O(nm \log(nm))$  time and  $O(nm)$  space.*

### 2.3 An output-sensitive algorithm

We now show that, performing a plane sweep using a *sweeping circle* centered at  $r$  whose diameter increases continuously, it is possible to intersect  $P$  and the set of rotation circles in a more efficient way. The idea is to maintain a list of the edges intersecting the *sweeping-circle*, ordered by appearance along the sweeping-circle. Using the same technique shown in Figure 3, the edges are labeled as defining in- or out- events. The algorithm is outlined next.

1. **Normalize  $P$ .** In the following steps, we consider  $P$  to have no edges intersecting any circle centered at  $r$  more than once. This can be guaranteed by performing a preprocessing step on  $P$ : For every edge  $e = uv$  of  $P$ , let  $p_e$  be the intersection point between the line  $\ell$  containing  $e$  and the line perpendicular to  $\ell$  passing through  $r$ . If  $p_e$  belongs to the relative interior of  $e$ , subdivide this edge into the edges  $up_e$  and  $p_ev$ . In the worst case, each edge of  $P$  gets subdivided into two parts. See Figure 5.

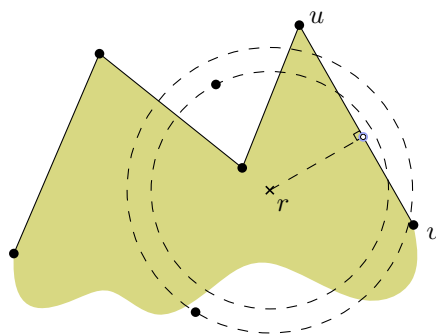


Figure 5: Splitting an edge of  $P$ .

2. **Process a vertex of  $P$ .** Sort first the vertices of  $P$  and  $S$  according to their distance from  $r$ . This is the order in which an expanding sweeping circle centered at  $r$  will reach them.

As the sweeping-circle increases in size, we stop at each vertex  $p_j$  of  $P$ . Each time this happens, the number of intersections of  $C_{p_j}(r)$  with the boundary of  $P$  will increase or decrease by two. We can maintain and update the ordered list of edges intersected by  $C_{p_j}(r)$ , using a red-black tree, in logarithmic time. This enables us to calculate the intersections of  $C_{p_j}(r)$  in time proportional to their number. It suffices to walk along the ordered list of edges intersected by the sweeping-circle. Each time the sweeping circle reaches an element of  $S$ , the number and order of intersections of the sweeping circle with the edges of  $P$  remains unchanged. However, since the points of intersection change, we need to recalculate them each time we reach a point of  $P$  or  $S$ .

3. **Compute the intervals sequence for each element of  $S$ .** We can now compute, within the same time complexity, the intervals in which  $C_{p_j}(r)$  intersects the interior of  $P$ . Note that these intervals are not the elements of  $\mathcal{I}_j$ , they have to be rotated according to the position of  $p_j$  with respect to  $r$ .
4. **Construct the events sequence.** Since for each point  $p_j$  in  $S$  we have computed the corresponding sequence of sorted intervals  $\mathcal{I}_j$ , all

we need to do is to merge these (at most  $n$ ) sequences into a complete sequence of events.

The normalization process takes  $O(m)$  time. Sorting the points in  $S$  and the vertices of  $P$  by distance from  $r$  takes  $O(n \log n)$  and  $O(m \log m)$  time, respectively. The ordered list of edges intersecting the sweep-line is maintained in an  $O(m)$ -size red-black tree, so we can process all the vertices of  $P$  in  $O(m \log m)$  time. On the other hand, processing all the points in  $S$  takes  $O(k)$  time, where  $k$  denotes the total number of in- and out-events in a Fixed MCR problem. Finally, merging the  $O(n)$  sequences of sorted intervals takes  $O(k \log n)$  time. We then sweep the merged list of  $\mathcal{I}_1 \cup \dots \cup \mathcal{I}_n$  in  $O(k)$  time to obtain a solution to our problem. The total time complexity is  $O(n \log n + m \log m + k \log n)$ . The space complexity is  $O(n + m + k)$ . We have thus proved:

**Theorem 6.** *The Fixed MCR problem can be solved in  $O((n + k) \log n + m \log m)$  time and  $O(n + m + k)$  space.*

### 3 Segment-restricted MCR (Problem 2)

Our approach to solve Problem 2 is to characterize, for each  $p$  in  $S$ , the intersection between the polygon  $P$  and the rotation circle  $C_p(r)$  while the center  $r$  of  $C_p(r)$  moves along a line segment  $\ell = \overline{ab}$  from  $a$  to  $b$ . For simplicity, we assume that  $a$  lies on the origin  $(0, 0)$  and  $b$  on the positive  $x$ -axis. For each edge  $e = \overline{uv}$  of  $P$ , we parameterize the intersection between  $C_p(r)$  and  $e$  using a function  $\omega = f(x)$ , where  $x$  is the  $x$ -coordinate of  $r$  (ranging from 0 to the  $x$ -coordinate  $b.x$  of  $b$ ) and  $\omega$  is the counterclockwise angle swept by the ray  $\overrightarrow{rp}$  until it coincides with the ray emanating from  $r$  and passing through the current point of intersection  $q$  of  $C_p(r)$  and  $e$  (assume for the moment that there exists exactly one such point of intersection). See Figure 12.

Leaving the details for Section 3.4, we obtain the following expression of  $\omega$  as a function of  $x$ :

$$\omega = \arccos \left( \frac{\gamma(x) \pm \sqrt{\delta(x)}}{\epsilon(x)} \right), \quad (1)$$

where  $\gamma(x)$ ,  $\delta(x)$ , and  $\epsilon(x)$  are polynomials of degrees 2, 4, and 2, respectively. The motion of  $r$  along  $\ell$  thus corresponds to a set of points  $(x, \omega)$  for which  $p$  hits the boundary of  $P$ . For each point  $p \in S$ , these points form  $O(m)$  curves bounding a collection of simple regions in the  $x$ - $\omega$  plane; each point  $(x, \omega)$  of any such region corresponds to a rotation of  $p$ , by a counterclockwise angle of size  $\omega$  with respect to a rotation center at  $(x, 0)$ , for which  $p$  belongs to  $P$ . Note that each pair of such regions have disjoint interiors,

whereas their boundaries may intersect at most at a common vertex due to the simplicity of  $P$ .

### 3.1 Subdividing the Edges of the Polygon

We mentioned earlier that, for convenience, we subdivide the edges of the polygon  $P$  about their points of intersection (if any) with the  $x$ -axis; so, in the following, we assume that each edge has no points on either side of the  $x$ -axis. We further subdivide the edges in order to simplify the computation of the angle  $\omega$  in terms of the  $x$ -coordinate of the rotation center  $r$  as it moves along the segment  $\overline{ab}$ .

**Theoretical Framework.** Let us consider that we process the point  $p \in S$ , and denote by  $D_p(r)$  the closed disk bounded by  $C_p(r)$ , where  $r$  is a point in  $\overline{ab}$ . In Figure 7,  $p$  is taken to lie above the  $x$ -axis where either  $a.x \leq p.x \leq b.x$  (top figure) or  $b.x < p.x$  (bottom figure). The cases where  $p.x < a.x$  or where  $p$  lies below the  $x$ -axis are symmetric, whereas the case where  $p$  lies on the  $x$ -axis is similar (see figures 9 and 10). Moreover, let  $p'$  be the mirror image of  $p$  with respect to the  $x$ -axis; clearly,  $p'$  coincides with  $p$  if  $p$  lies on the  $x$ -axis. Finally, let  $H_p^L$  ( $H_p^R$ , resp.) be the open halfplane to the left (right, resp.) of the line perpendicular to the  $x$ -axis that passes through  $p$ .

Then, it is useful to observe the following properties.

**Lemma 7.** *Let  $p$  be a point, and let  $H_p^L$ ,  $H_p^R$ ,  $C_p(r)$ , and  $D_p(r)$ , for  $r \in \overline{ab}$ , be as defined above.*

- (i) *Consider any two points  $r, r' \in \overline{ab}$  with  $r \neq r'$ . If the point  $p$  lies on the  $x$ -axis, then the circles  $C_p(r), C_p(r')$  intersect only at  $p$ . If the point  $p$  does not lie on the  $x$ -axis, the circles  $C_p(r), C_p(r')$  intersect at  $p$  and at  $p$ 's mirror image  $p'$  about the  $x$ -axis, and the line segment  $\overline{pp'}$  belongs to both  $D_p(r), D_p(r')$ .*
- (ii)  $\triangleright$  *For every point  $s$  in the interior of  $H_p^L \cap D_p(r)$ , there exists a unique circle centered on the  $x$ -axis that passes from  $p$  and  $s$  and its center lies to the right of  $r$ ;*
- $\triangleright$  *for every point  $t$  in  $H_p^L - D_p(r)$ , there exists a unique circle centered on the  $x$ -axis that passes from  $p$  and  $t$  and its center lies to the left of  $r$ .*

*Symmetrically,*

- $\triangleright$  *for every point  $s'$  in the interior of  $H_p^R \cap D_p(r)$ , there exists a unique circle centered on the  $x$ -axis that passes from  $p$  and  $s'$  and its center lies to the left of  $r$ ;*



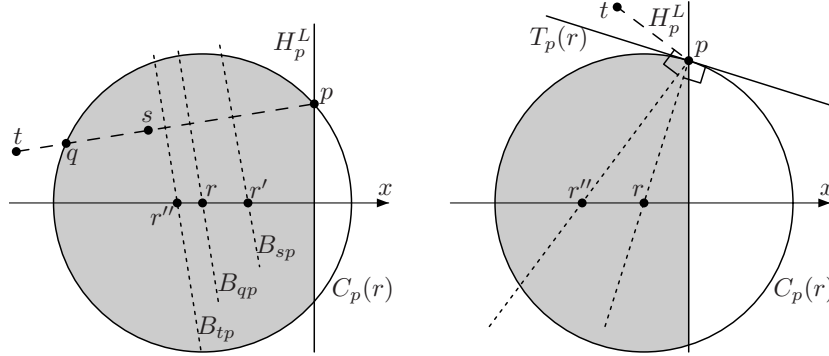


Figure 6: For the proof of Lemma 7. (left) The perpendicular bisectors  $B_{sp}$ ,  $B_{qp}$ ,  $B_{tp}$  intersect the  $x$ -axis at points  $r'$ ,  $r$ ,  $r''$ , respectively. (right) The lines through  $p$  that are perpendicular to the tangent at  $p$  and to  $\overline{tp}$  intersect the  $x$ -axis at points  $r$ ,  $r''$ , respectively.

▷ for every point  $t'$  in  $H_p^R - D_p(r)$ , there exists a unique circle centered on the  $x$ -axis that passes from  $p$  and  $t'$  and its center lies to the right of  $r$ .

*Proof.*

(i) From the definition of the circles  $C_p(r)$  for all  $r \in \overline{ab}$ ,  $p$  belongs to each such circle.

Next, assume that  $p$  lies on the  $x$ -axis and suppose for contradiction that two circles  $C_p(r), C_p(r')$  with  $r \neq r'$  intersect at a point  $p' \neq p$  as well. Then, both  $r, r'$  would belong to the perpendicular bisector of the line segment  $\overline{pp'}$ ; thus, the perpendicular bisector should coincide with the  $x$ -axis. Then, since  $p$  lies on the  $x$ -axis,  $p'$  would coincide with  $p$ , in contradiction to the assumption that  $p' \neq p$ . Therefore, if  $p$  lies on the  $x$ -axis, any two circles  $C_p(r), C_p(r')$  with  $r \neq r'$  intersect only at  $p$ .

Now, assume that  $p$  does not lie on the  $x$ -axis. Then, since  $p'$  is the mirror image of  $p$  with respect to the  $x$ -axis, the  $x$ -axis is the perpendicular bisector of the segment  $\overline{pp'}$ . Thus,  $p'$  belongs to all the circles centered on the  $x$ -axis that pass from  $p$ . The fact that  $\overline{pp'}$  belongs to each of the disks  $D_p(r)$ , for all  $r \in \overline{ab}$ , follows from the fact that each disk  $D_p(r)$  is a convex set containing  $p$  and  $p'$ .

(ii) Let  $q$  be the point of intersection of  $C_p(r)$  with the line  $L$  through  $p$  and  $s$ ; see Figure 6(left). The line  $L$  is well defined since  $s \neq p$ . In fact,  $s.x < p.x$  (because  $s$  belongs to  $H_p^L$ ), and thus  $L$  is not perpendicular to the  $x$ -axis, which implies that the perpendicular bisector  $B_{qp}$  of the line segment  $\overline{qp}$  intersects the  $x$ -axis at a single point; this point of intersection

is precisely the center  $r$  of  $C_p(r)$ . Since the perpendicular bisector of the line segment  $\overline{sp}$  is parallel to  $B_{qp}$  and lies to the right of  $B_{qp}$  (because  $s$  is an interior point of  $\overline{qp}$ ), it intersects the  $x$ -axis at a single point  $r'$  to the right of  $r$ ;  $r'$  is the center of the circle centered on the  $x$ -axis that passes from  $p$  and  $s$ .

Now, consider  $t \in H_p^L - D_p(r)$ , and let  $T_p(r)$  be the open halfplane that is tangent to the circle  $C_p(r)$  at  $p$  and contains  $r$ . If  $t \in T_p(r)$ , then the line  $L$  through  $p$  and  $t$  intersects  $C_p(r)$  at  $p$  and at another point  $q$ , and  $q \in \overline{tp}$ . Then, as above, the perpendicular bisector  $B_{qp}$  of  $\overline{qp}$  intersects the  $x$ -axis at  $r$ , whereas the perpendicular bisector of  $\overline{tp}$  is parallel and to the left of  $B_{qp}$  (since  $q$  is an interior point of  $\overline{tp}$ ), and thus intersects the  $x$ -axis at a point  $r''$  to the left of  $r$ ; see Figure 6(left). It is important to observe that the proof so far applies no matter whether  $p$  lies on the  $x$ -axis or not.

Next, let us consider the case in which  $t \notin T_p(r)$ ; this case is not possible if  $p$  lies on the  $x$ -axis since then  $T_p(r) = H_p^L$ . Then, the line through  $p$  perpendicular to the tangent to the circle  $C_p(r)$  at  $p$  intersects the  $x$ -axis at  $r$ . Since  $t \notin T_p(r)$ , the line perpendicular to the line through  $t$  and  $p$  is not parallel to the  $x$ -axis and thus intersects the  $x$ -axis at a single point  $r''$ . In fact, since the angle  $\widehat{tpr}$  of the triangle with  $t, p, r$  as vertices is larger than  $\pi/2$ ,  $r''$  is to the left of  $r$ ; see Figure 6(right).

The results for points  $s'$  in the interior of  $H_p^R \cap D_p(r)$  and  $t' \in H_p^R - D_p(r)$  are obtained in a fashion left-to-right symmetric to the one we used in order to obtain the results for the points  $s$  in the interior of  $H_p^L \cap D_p(r)$  and  $t \in H_p^L - D_p(r)$ , respectively.  $\square$

Statement (ii) of Lemma 7 directly implies that the union of all the circles  $C_p(r)$  forms precisely the closure of the symmetric difference  $D_p(a) \oplus D_p(b)$  of the disks  $D_p(a)$  and  $D_p(b)$  centered at  $a$  and  $b$ , respectively (see Figure 7); note that any point in the interior of

$$\left( (D_p(a) - D_p(b)) \cap H_p^L \right) \cup \left( (D_p(b) - D_p(a)) \cap H_p^R \right)$$

lies on a circle  $C_p(r)$  with  $r$  in the interior of  $\overline{ab}$ , whereas no other point does so. Lemma 7(ii) also implies the following corollary.

**Corollary 8.**

(i) For any  $r, r' \in \overline{ab}$  with  $r$  to the left of  $r'$ :

$$\begin{aligned} &\triangleright (C_p(r) \cap D_p(r')) \cap H_p^L = \emptyset \quad \text{and} \quad D_p(r') \cap H_p^L \subset D_p(r) \cap H_p^L; \\ &\triangleright (C_p(r') \cap D_p(r)) \cap H_p^R = \emptyset \quad \text{and} \quad D_p(r) \cap H_p^R \subset D_p(r') \cap H_p^R. \end{aligned}$$

(ii) Suppose that a line segment  $I$  intersects a circle  $C_p(r)$ , where  $r \in \overline{ab}$ , at points  $w_1, w_2$  such that the line segment  $\overline{w_1 w_2}$  lies entirely in the closure of  $(D_p(a) - D_p(b))$ . Then, the segment  $I$  is tangent to

a circle  $C_p(r')$  for some  $r' \in \overline{ab}$  and the point of tangency belongs to  $\overline{w_1w_2}$ . Symmetrically, the same result holds if the segment  $\overline{w_1w_2}$  lies entirely in the closure of  $(D_p(b) - D_p(a))$ .

*Proof.*

(i) We prove the propositions for the halfplane  $H_p^L$ ; the proofs for  $H_p^R$  are left-to-right symmetric.

Since  $r$  is to the left of  $r'$ , Lemma 7(ii) implies that  $C_p(r') \cap H_p^L$  lies in the interior of  $D_p(r) \cap H_p^L$ . This in turn implies that (i)  $(C_p(r) \cap H_p^L) \cap (D_p(r') \cap H_p^L) = \emptyset$ , i.e.,  $(C_p(r) \cap D_p(r')) \cap H_p^L = \emptyset$ , and (ii)  $(D_p(r') \cap H_p^L) \subset (D_p(r) \cap H_p^L)$  since the disk  $D_p(r')$  is bounded by  $C_p(r')$  and since each such disk is a convex set; we have a proper subset relation because the points in  $C_p(r) \cap H_p^L$  do not belong to  $D_p(r') \cap H_p^L$ .

(ii) Below, we prove the statement for the case that  $\overline{w_1w_2}$  lies entirely in the closure of  $(D_p(a) - D_p(b))$ ; the proof for the case that  $\overline{w_1w_2} \in \text{closure}(D_p(b) - D_p(a))$  is left-to-right symmetric.

Since  $w_1 \neq w_2$  and  $\overline{w_1w_2} \in \text{closure}(D_p(a) - D_p(b))$ , then  $r \neq b$ ; let  $t \in \overline{ab}$  be a point infinitesimally to the right of  $r$ . Then, according to statement (i),  $(C_p(r) \cap D_p(t)) \cap H_p^L = \emptyset$  and  $(D_p(t) \cap H_p^L) \subset (D_p(r) \cap H_p^L)$ , which together imply that  $(D_p(t) \cap I) \subset \overline{w_1w_2}$ ; note that at least one of  $w_1, w_2$  (which belong to  $C_p(r)$ ) belongs to  $H_p^L$ , for otherwise, either  $\overline{w_1w_2}$  degenerates to a single point, in contradiction to the fact that  $w_1 \neq w_2$ , or  $\overline{w_1w_2} = \overline{pp'}$  with  $p \neq p'$ , in contradiction to the fact that  $\overline{w_1w_2}$  lies entirely in the closure of  $(D_p(a) - D_p(b))$ . Since the rotation center moves continuously along  $\overline{ab}$  there exists a point  $r' \in \overline{rb}$  such that  $D_p(r') \cap I$  is a single point, i.e., the line segment  $I$  is tangent to the circle  $C_p(r')$ ; moreover, since  $D_p(r') \cap I \subset \overline{w_1w_2}$ , the point of tangency belongs to the line segment  $\overline{w_1w_2}$ .  $\square$

**The Subdivision Procedure.** Our subdivision procedure for the polygon edges while processing point  $p \in S$  works in two phases: in Phase 1, we ensure that each circle  $C_p(r)$  intersects each resulting sub-edge in at most one point; in Phase 2, we ensure that for each sub-edge either  $0 \leq \omega \leq \pi$  or  $\pi \leq \omega \leq 2\pi$  implying that the value of  $\omega$  is uniquely determined from the value of its cosine.

*Phase 1:* If an edge  $\overline{uv}$  of the polygon  $P$  does not intersect  $D_p(a) \cup D_p(b)$  or if at least one of its endpoints belongs to  $D_p(a) \cap D_p(b)$ , then we need not do anything, otherwise:

- If  $\overline{uv}$  does not intersect the interior of  $D_p(a) \cap D_p(b)$ , then  $\overline{uv}$  is tangent to at most two of the circles  $C_p(r)$  and we subdivide it at these points of tangency; see edges  $\overline{u_1v_1}$  and  $\overline{u_2v_2}$  in Figure 7.

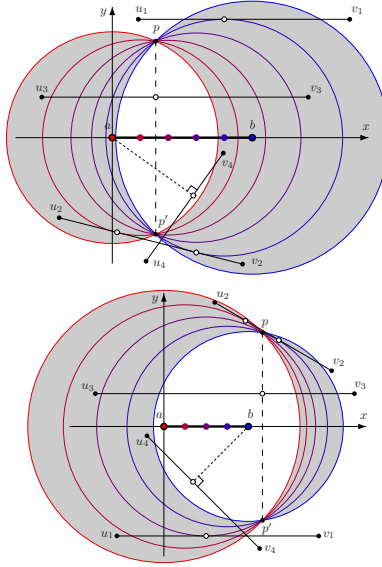


Figure 7: Subdividing the polygon edges so that each sub-edge is intersected at most once by each of the circles  $C_p(r)$  (white disks denote points of edge subdivision).

- If  $\overline{uv}$  intersects the interior of  $D_p(a) \cap D_p(b)$ , then it crosses  $D_p(a) \cap D_p(b)$ . If  $\overline{uv}$  intersects the segment  $\overline{pp'}$ , then we subdivide  $\overline{uv}$  at its point of intersection with  $\overline{pp'}$  (see edge  $\overline{u_3v_3}$  in Figure 7); if not, then the points of intersection of  $\overline{uv}$  with the boundary of  $D_p(a) \cap D_p(b)$  both belong to either  $C_p(a)$  or  $C_p(b)$  (see edge  $\overline{u_4v_4}$  in Figure 7), in which case we subdivide  $\overline{uv}$  at its closest point to  $a$  or  $b$ , respectively.

It is not difficult to see that if the edge  $\overline{uv}$  has two points of intersection with a circle  $C_p(r)$ , these two points of intersection end up belonging to different parts of the subdivided edge.

After Phase 1 has been complete, we apply Phase 2 on the resulting sub-edges. Let  $a'$  and  $b'$  be points such that  $a$  and  $b$  are the midpoints of segments  $\overline{pa'}$  and  $\overline{pb'}$ , respectively; see Figure 8. Then, Phase 2 involves the following subdivision steps.

*Phase 2:*

- If a sub-edge intersects  $\overline{a'b'}$ , we subdivide it at this point of intersection (in Figure 8, see sub-edges  $\overline{u_1v_1}$  and sub-edge  $\overline{u_2v_2}$  in the top figure).
- Additionally, if the sub-edge is tangent to two circles, we subdivide it at its point of intersection with the line through  $p$  perpendicular to the  $x$ -axis (see sub-edges  $\overline{u_2v_2}$  in Figure 8).

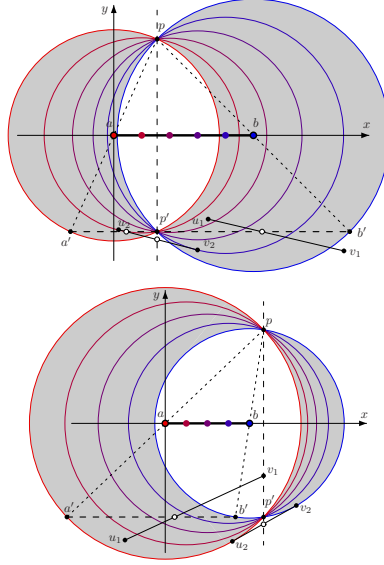


Figure 8: Further subdividing the polygon edges so that the angle  $\omega$  belongs either to  $[0, \pi]$  or to  $[\pi, 2\pi]$  (white disks denote points of edge subdivision).

By taking into account that each of Phase 1 and Phase 2 may introduce at most two subdivision points on a polygon edge, we conclude that each edge ends up subdivided into at most 5 sub-edges.

Finally, it is important to note that the above described edge subdivision is introduced precisely for the processing of the current point  $p \in S$  being processed; that is, for the next element of  $S$ , we ignore the subdivision points introduced and start working again with the edges of the polygon  $P$  (subdivided only about the  $x$ -axis).

**Correctness.** Before proving Theorem 10 which establishes the correctness of the subdivision procedure, we show the following useful lemma.

**Lemma 9.** *Let  $p$  be an element of the point set  $S$  and  $p'$  be the mirror image of  $p$  with respect to the  $x$ -axis.*

- (i) *If the point  $p$  is such that  $0 = a.x \leq p.x \leq b.x$ , then  $p'$  belongs to the line segment  $\overline{a'b'}$ .*
- (ii) *For any point  $q \in \overline{a'b'}$  such that  $q \neq p'$ , there is a point  $r \in \overline{ab}$  for which  $C_p(r)$  has the segment  $\overline{qp}$  as its diameter.*

*Proof.*

(i) First, assume that  $p$  lies on the  $x$ -axis. Then,  $p' = p$ . The assumption  $a.x \leq p.x \leq b.x$  implies that  $p \in \overline{ab}$ , which in turn implies that  $\overline{ab} \subset \overline{a'b'}$ ; see

Figure 10. Thus,  $p \in \overline{a'b'}$ , i.e.,  $p' = p \in \overline{a'b'}$ . Now, consider the case that  $p$  does not lie on the  $x$ -axis. Let  $c$  be the (vertical) projection of  $p$  onto the  $x$ -axis. Since  $a.x \leq p.x \leq b.x$ ,  $c \in \overline{ab}$ . The line defined by  $p, c$  (note that  $p \neq c$ ) is perpendicular to the  $x$ -axis and let  $d$  be its point of intersection with the line supporting  $\overline{a'b'}$ . Since  $c \in \overline{ab}$ , we conclude that  $d \in \overline{a'b'}$ . Moreover, by its construction, the line segment  $\overline{a'd'}$  is parallel to the  $x$ -axis, and since  $|\overline{pa}| = |\overline{aa'}|$ , the similarity of the triangles with vertices  $p, a, c$  and  $p, a', d$  implies that  $|\overline{pc}| = |\overline{cd}|$ . Thus,  $p' = d$  and hence  $p' \in \overline{a'b'}$ .

(ii) Assume that  $p$  lies on the  $x$ -axis. Let  $q \in \overline{a'b'}$  with  $q \neq p$ , and suppose without loss of generality that  $q$  is to the left of  $p$  (the case where  $q$  is to the right of  $p$  is symmetric). Then, the midpoint of  $\overline{qp}$  lies in  $\overline{ap}$  and it is the center of the unique circle  $C_p(r)$  passing through  $q$ . Therefore,  $C_p(r)$  has  $\overline{qp}$  as its diameter.

Now assume that  $p$  does not lie on the  $x$ -axis. Consider any point  $q \in \overline{a'b'}$  with  $q \neq p'$ . Let  $z$  be the point of intersection of the line segment  $\overline{pq}$  with the  $x$ -axis ( $z$  exists because  $p$  and  $\overline{a'b'}$ , and hence  $p$  and  $q$ , lie on opposite sides of the  $x$ -axis). Note that  $z \in \overline{ab}$  since  $q \in \overline{a'b'}$ . Then, by the similarity of the triangles  $\triangle paz$  and  $\triangle pa'q$  we have that  $|\overline{pz}| = |\overline{zq}|$ ; i.e., the point  $z$  is the midpoint of  $\overline{pq}$ . Therefore,  $z$  belongs to the perpendicular bisector of  $\overline{pq}$  and in fact, it is the only point of intersection of such bisector and the  $x$ -axis. Note that, since  $q \neq p'$ , the line passing through  $p$  and  $q$  (remember that  $p \neq q$ ) is not perpendicular to the  $x$ -axis. This implies that the center  $r$  of any circle  $C_p(r)$  passing through  $q$  coincides with  $z$ , that is,  $\overline{qp}$  is a diameter of  $C_p(r)$ .  $\square$

Lemma 9(ii) implies that for any point  $q \neq p'$  belonging to  $\overline{a'b'}$ , the corresponding angle  $\omega = \widehat{prq}$  is equal to  $\pi$ , where  $r \in \overline{ab}$  is the center of the circle  $C_p(r)$  passing from  $q$ .

Now we are ready to prove Theorem 10 which establishes that the subdivision steps of Phases 1 and 2 achieve the set goals.

**Theorem 10.**

- (i) *After the completion of Phase 1, no resulting sub-edge intersects any circle  $C_p(r)$  for some  $r \in \overline{ab}$  in more than one point.*
- (ii) *After the completion of Phase 2, for any two points  $q, q'$  (lying on circles  $C_p(r)$  and  $C_p(r')$ , respectively) of each resulting sub-edge, the counterclockwise angles  $\widehat{prq}$  and  $\widehat{pr'q'}$  either both belong to  $[0, \pi]$  or both belong to  $[\pi, 2\pi]$ .*

*Proof.*

(i) Suppose for contradiction that there exists a sub-edge  $\overline{cd}$  and a circle  $C_p(r)$  with  $r \in \overline{ab}$  that intersect in two points  $w_1$  and  $w_2$ . The point  $p$  and its mirror image  $p'$  subdivide the circle  $C_p(r)$  into two arcs,  $A_p^L$  and  $A_p^R$ , the former to the left of the line through  $p$  perpendicular to the  $x$ -axis and the latter to the right (note that if  $p$  lies on the  $x$ -axis, one of these arcs degenerates into a single point). Then,  $w_1, w_2$  should belong to the same arc; otherwise,  $p$  would not lie on the  $x$ -axis and the line segment  $\overline{w_1w_2}$  would intersect the line segment  $\overline{pp'}$ , and thus the sub-edge  $cd$  would have been subdivided in Phase 1 about its point of intersection with  $\overline{pp'}$ . Suppose without loss of generality that  $w_1, w_2$  belong to the arc  $A_p^L$ . But then, no matter whether the segment  $\overline{w_1w_2}$  intersects the interior of  $D_p(a) \cap D_p(b)$  or not, we have a contradiction. In the former case, the sub-edge  $cd$  would have been subdivided in Phase 1 about the perpendicular projection of  $b$  onto  $cd$ ;  $b$ 's projection onto  $cd$  belongs to  $D_p(a) \cap D_p(b)$  and thus is an interior point of  $\overline{w_1w_2}$ . In the latter case, the sub-edge  $cd$  would have been subdivided in Phase 1 about its point of tangency with a circle  $C_p(t)$  with  $t \in \overline{ab}$ ; this point of tangency belongs to  $\overline{w_1w_2}$  as shown in Corollary 8(ii). Therefore, after Phase 1, no resulting sub-edge intersects any circle  $C_p(r)$  for some  $r \in \overline{ab}$  in more than one point.

(ii) Suppose without loss of generality that the point  $p$  lies above or on the  $x$ -axis and it holds that  $p.x \geq a.x$ ; the case where it holds that  $p.x < a.x$  is left-to-right symmetric (the corresponding angles are equal to  $2\pi$  minus the corresponding angles when  $p.x > b.x$ ), whereas the case where  $p$  lies below the  $x$ -axis is top-down symmetric (in this case too, the corresponding angles are equal to  $2\pi$  minus the corresponding angles when  $p$  lies above the  $x$ -axis).

Let  $R_1$  ( $R_3$ , respectively) be the subsets of points in the closure of the symmetric difference  $D_p(a) \oplus D_p(b)$  that are on or to the left of the line through  $p$  that is perpendicular to the  $x$ -axis and are on or above (on or below, respectively)  $\overline{a'b'}$ ; symmetrically, let  $R_2$  ( $R_4$ , respectively) be the subsets of points in the closure of the symmetric difference  $D_p(a) \oplus D_p(b)$  that are on or to the right of the line through  $p$  that is perpendicular to the  $x$ -axis and are on or above (on or below, respectively)  $\overline{a'b'}$ ; see Figure 9 and Figure 10. Consider a point  $w$  lying on a circle  $C_p(t)$  with  $t \in \overline{ab}$ . Since according to Lemma 9(ii), for any point  $q \in \overline{a'b'}$ , the segment  $\overline{qp}$  is a diameter of the circle centered on the  $x$ -axis and passing from  $p, q$ , if  $w \in R_1$ , the counterclockwise angle  $\widehat{ptw}$  belongs to  $[0, \pi]$ . Similarly, if  $w \in R_2$  then  $\widehat{ptw} \in [\pi, 2\pi]$ , if  $w \in R_3$  then  $\widehat{ptw} \in [\pi, 2\pi]$ , and if  $w \in R_4$  then  $\widehat{ptw} \in [0, \pi]$ . Since no sub-edge resulting after Phase 2 contains points in more than one of the regions  $R_1, R_2, R_3, R_4$ , the statement of the theorem follows.  $\square$

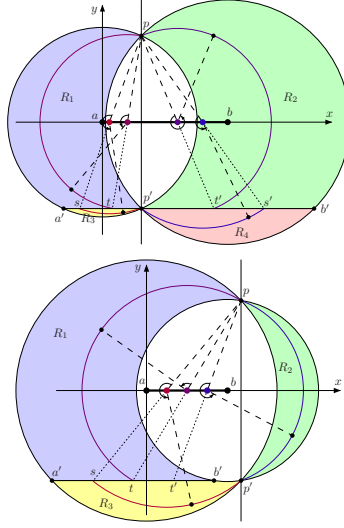


Figure 9: The partition of the closure of the symmetric difference  $D_p(a) \oplus D_p(b)$  about the line segment  $\overline{a'b'}$  and the line defined by  $p, p'$  into regions  $R_1, R_2, R_3, R_4$  when the point  $p$  does not lie on the  $x$ -axis. Note that the line segments  $ps, ps', pt, pt'$  are diameters.

### 3.2 The Algorithm

We are now ready to outline our algorithm for Problem 2:

1. **Subdivide the edges of polygon  $P$  about the  $x$ -axis.**
2. **Process each point  $p \in S$ .** For each point  $p$ , we subdivide each edge of polygon  $P$  (resulting from the previous step) into sub-edges (see the edge subdivision process described earlier). Next, for each sub-edge, we compute the curve of the angle  $\omega$  with respect to the  $x$ -coordinate  $x$  of the rotation center as it moves along  $\overline{ab}$  (see Equation 1), and finally we form the regions bounded by these curves.
3. **Construct and traverse the arrangement of all the regions.** Using standard techniques, we construct the arrangement of all the regions of all the elements of  $S$ . Next, we traverse the dual graph of the resulting arrangement looking for a sub-region of maximum depth; any point in this sub-region determines a position  $(x, 0)$  of  $r$  and a rotation angle  $\omega$  that constitute a solution to the problem.

### 3.3 Time and Space Complexity

Step 1 clearly takes  $O(m)$  time and space, resulting into at most  $2m$  sub-edges. The edge subdivision while processing a point  $p \in S$  in Step 2 takes



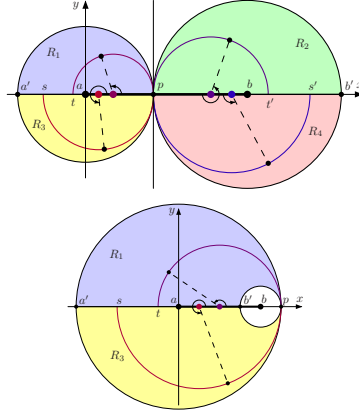


Figure 10: The partition of the closure of the symmetric difference  $D_p(a) \oplus D_p(b)$  about the line segment  $\overline{a'b'}$  and the line that is perpendicular to the  $x$ -axis at  $p$  into regions  $R_1, R_2, R_3, R_4$  when the point  $p$  lies on the  $x$ -axis. Note that the line segments  $ps, ps', pt, pt'$  are diameters.

$O(m)$  time and space, producing  $O(m)$  sub-edges: For each sub-edge  $\overline{uv}$ ,  $O(1)$  time suffices to determine whether its endpoints belong to the disks  $D_p(a)$  and  $D_p(b)$ , and whether  $\overline{uv}$  intersects the circles  $C_p(a), C_p(b)$ , the segment  $\overline{pp'}$ , or the line supporting  $\overline{pp'}$ , as well as to compute any points of intersection. Moreover, the centers of the circles  $C_p(r)$ , for  $r \in \overline{ab}$ , to which  $\overline{uv}$  is tangent are precisely the points of intersection of the segment  $\overline{ab}$  with the parabola that is equidistant from point  $p$  and the line supporting  $\overline{uv}$ . Then, processing  $p$  yields  $O(m)$  curves bounding  $O(m)$  regions. Thus, processing all the points in  $S$  in Step 2 takes a total of  $O(nm)$  time and produces a set of  $O(nm)$  regions bounded by  $O(nm)$  curves in the  $x$ - $\omega$  plane. From Step 1, we can show the following lemma:

**Lemma 11.** *Any two  $(\omega$ - $x$ )-curves as in Equation 1 have at most 32 points of intersection.*

*Proof.* The idea is based on the fact that a polynomial of constant degree has a constant number of roots. In our case, we have a square root which needs to be squared in order to be removed. Let us consider the two  $(\omega$ - $x$ )-curves

$$\omega = \arccos\left(\frac{\gamma_1(x) \pm \sqrt{\delta_1(x)}}{\epsilon_1(x)}\right) \quad \text{and} \quad \omega = \arccos\left(\frac{\gamma_2(x) \pm \sqrt{\delta_2(x)}}{\epsilon_2(x)}\right).$$

Since a point of intersection of these curves belongs to both of them, we have:

$$\omega = \arccos\left(\frac{\gamma_1(x) \pm \sqrt{\delta_1(x)}}{\epsilon_1(x)}\right) = \arccos\left(\frac{\gamma_2(x) \pm \sqrt{\delta_2(x)}}{\epsilon_2(x)}\right)$$

$$\implies \gamma_1(x) \epsilon_2(x) - \gamma_2(x) \epsilon_1(x) = \pm \left( \epsilon_2(x) \sqrt{\delta_1(x)} - \epsilon_1(x) \sqrt{\delta_2(x)} \right) \quad (2)$$

from which, by squaring twice to get rid of the square roots, we get

$$\begin{aligned} \left( \gamma_1(x) \epsilon_2(x) - \gamma_2(x) \epsilon_1(x) \right)^2 &= \left( \epsilon_2(x) \sqrt{\delta_1(x)} - \epsilon_1(x) \sqrt{\delta_2(x)} \right)^2 \\ \implies \left( \gamma_1(x) \epsilon_2(x) - \gamma_2(x) \epsilon_1(x) \right)^2 - \epsilon_2^2(x) \delta_1(x) - \epsilon_1^2(x) \delta_2(x) & \\ &= -2 \epsilon_1(x) \epsilon_2(x) \sqrt{\delta_1(x) \delta_2(x)} \\ \implies \left( \left( \gamma_1(x) \epsilon_2(x) - \gamma_2(x) \epsilon_1(x) \right)^2 - \epsilon_2^2(x) \delta_1(x) - \epsilon_1^2(x) \delta_2(x) \right)^2 & \\ &= 4 \epsilon_1^2(x) \epsilon_2^2(x) \delta_1(x) \delta_2(x). \quad (3) \end{aligned}$$

The last equality is a polynomial of degree at most 16 and, thus, it has at most 16 real roots for  $x$  (it is important to note that the value of  $x$  in any pair  $(\omega, x)$  satisfying Equation 2 satisfies the polynomial in Equation 3, although the reverse does not necessarily hold, i.e., not every root of the polynomial satisfies Equation 2). Thus, if we substitute the real roots of the polynomial in Equation 3 into Equation 1, we get at most 32 possible points of intersection, due to the  $\pm$  operand.  $\square$

Hence, the total number of intersection points of all the curves is  $O(n^2 m^2)$ . Using standard techniques, in  $O(n^2 m^2 \log(nm))$  time the arrangement of all these regions can be computed, and the dual graph of the resulting arrangement can be traversed looking for a sub-region of maximum depth. Any point in this sub-region determines a position of the rotation center  $r$  and a rotation angle  $\omega$  that constitute a solution to the problem. The space complexity is  $O(n^2 m^2)$ . Then:

**Theorem 12.** *The Segment-restricted MCR problem can be solved in  $O(n^2 m^2 \log(nm))$  time and  $O(n^2 m^2)$  space.*

Note that Problem 2 can also be solved in  $O(n^2 m^2 \log(nm))$  time even when the rotation center is restricted to lie on a line  $L$ : Compute the Voronoi diagram of  $P \cup S$ , and apply the algorithm we just described to a segment of  $L$  containing all the intersection points of  $L$  and the Voronoi edges. Moreover, if we restrict the rotation center to lie on a polygonal chain with  $s$  line segments, we can trivially obtain the optimal placement of  $P$  using  $O(sn^2 m^2 \log(nm))$  time. In both cases, the space complexity is  $O(n^2 m^2)$ .

### 3.4 Equation 1: expressing $w$ as a function of $x$

In order to simplify the exposition leading to Equation 1, for each point  $s$  in the plane other than the current rotation center  $r$ , we define a corresponding

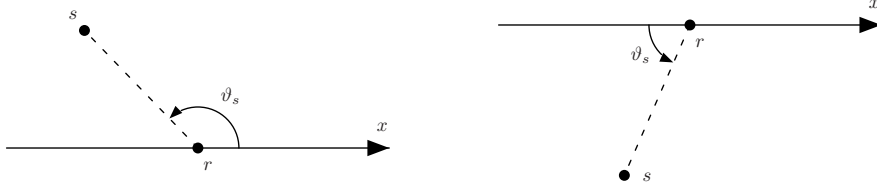


Figure 11: The definition of the angle  $\vartheta_s$  for any point  $s \neq r$ .

angle  $\vartheta_s$  with respect to  $r$ . In particular, let  $H_{\uparrow}$  be the set of points above the  $x$ -axis or on the  $x$ -axis and to the right of  $r$  and let  $H_{\downarrow}$  be the set of points below the  $x$ -axis or on the  $x$ -axis and to the left of  $r$  (clearly, the sets  $H_{\uparrow}$  and  $H_{\downarrow}$  partition  $\mathbb{R}^2 - \{r\}$ ). Then,

- if  $s \in H_{\uparrow}$ ,  $\vartheta_s$  is the angle swept by the rightward horizontal ray emanating from  $r$  as it moves in counterclockwise direction around  $r$  until it coincides with the ray  $\vec{rs}$  (see Figure 11, left);
- if  $s \in H_{\downarrow}$ ,  $\vartheta_s$  is the angle swept by the leftward horizontal ray emanating from  $r$  as it moves in counterclockwise direction around  $r$  until it coincides with the ray  $\vec{rs}$  (see Figure 11, right).

(Note that for all points  $s$  on the  $x$ -axis,  $\vartheta_s = 0$ .) From the definition of  $\vartheta_s$ , it follows that in all cases

$$0 \leq \vartheta_s < \pi \quad (4)$$

(we consider counterclockwise and clockwise angles being positive and negative, respectively) and

$$\cos \vartheta_s = \frac{s.x - r.x}{d(s,r)} \operatorname{sgn}(s.y) \quad \sin \vartheta_s = \frac{|s.y|}{d(s,r)} = \frac{s.y}{d(s,r)} \operatorname{sgn}(s.y) \quad (5)$$

where  $d(s,r)$  denotes the distance of point  $s$  from the rotation center  $r$ ,  $p.x$  and  $p.y$  are respectively the  $x$ - and  $y$ -coordinates of a point  $p$ , and  $\operatorname{sgn}(s.y)$  is the sign of  $s.y$ .

Now, we distinguish two main cases:

- *Point  $p$  and the intersection point  $q$  of the circle  $C_p(r)$  and the edge  $e = \overline{uv}$  of  $P$  both belong to either  $H_{\uparrow}$  or  $H_{\downarrow}$  (see Figure 12(a)):* if  $\vartheta_p \leq \vartheta_q$  then

$$\omega = \vartheta_q - \vartheta_p \quad (6)$$

otherwise

$$\omega = (\pi - \vartheta_p) + \pi + \vartheta_q = 2\pi + \vartheta_q - \vartheta_p. \quad (7)$$

- Point  $p$  and the intersection point  $q$  of the circle  $C_p(r)$  and the edge  $e = \overline{uv}$  of  $P$  do not both belong to either  $H_{\uparrow}$  or  $H_{\downarrow}$  (see Figure 12(b)): in this case,

$$\omega = (\pi - \vartheta_p) + \vartheta_q = \pi + \vartheta_q - \vartheta_p. \quad (8)$$

It is important to observe that the definition of  $H_{\uparrow}$  and  $H_{\downarrow}$  ensures that the above expressions for  $\omega$  hold for all special cases in which at least one of  $p, q$  lies on the  $x$ -axis, as summarized in the following table.

		$p \in H_{\uparrow}$		$p \in H_{\downarrow}$	
		$p$ on $x$ -axis $\vartheta_p = 0$	$p$ above $x$ -axis $0 < \vartheta_p < \pi$	$p$ on $x$ -axis $\vartheta_p = 0$	$p$ below $x$ -axis $0 < \vartheta_p < \pi$
$q \in H_{\uparrow}$	$q$ on $x$ -axis $\vartheta_q = 0$	$\omega = 0$	$\omega = 2\pi - \vartheta_p$	$\omega = \pi$	$\omega = \pi - \vartheta_p$
	$q$ above $x$ -axis $0 < \vartheta_q < \pi$	$\omega = \vartheta_q$	Eq. (6), (7)	$\omega = \pi + \vartheta_q$	Eq. (8)
$q \in H_{\downarrow}$	$q$ on $x$ -axis $\vartheta_q = 0$	$\omega = \pi$	$\omega = \pi - \vartheta_p$	$\omega = 0$	$\omega = 2\pi - \vartheta_p$
	$q$ below $x$ -axis $0 < \vartheta_q < \pi$	$\omega = \pi + \vartheta_q$	Eq. (8)	$\omega = \vartheta_q$	Eq. (6), (7)

In all cases,  $\cos(\omega) = \cos(\vartheta_q - \vartheta_p) = \cos(\vartheta_q) \cos(\vartheta_p) + \sin(\vartheta_q) \sin(\vartheta_p)$  which, due to Equation 5 and to the fact that  $d(q, r) = d(p, r)$ , implies that

$$\begin{aligned} \cos(\omega) &= \frac{(q.x - x)(p.x - x) + q.y p.y}{d^2(p, r)} \operatorname{sgn}(q.y) \operatorname{sgn}(p.y) \\ &= \frac{(q.x - x)(p.x - x) + q.y p.y}{(p.x - x)^2 + (p.y)^2} \operatorname{sgn}(q.y) \operatorname{sgn}(p.y) \\ &= \frac{x^2 - (q.x + p.x)x + q.x p.x + q.y p.y}{x^2 - 2p.x x + (p.x)^2 + (p.y)^2} \operatorname{sgn}(q.y) \operatorname{sgn}(p.y). \end{aligned} \quad (9)$$

For convenience, we subdivide each edge that intersects the  $x$ -axis at this point of intersection so that the value of  $\operatorname{sgn}(q.y)$  is fixed at each sub-edge no matter where  $q$  is.

The coordinates  $q.x, q.y$  of intersection point  $q$  can be expressed in terms of  $x$  by taking into account that  $q$  belongs to the line supporting the edge  $\overline{uv}$  and that  $r$  is equidistant from  $q$  and  $p$ . The former implies that there exists a real number  $\lambda$  with  $0 \leq \lambda \leq 1$  such that the vector  $\overline{uq}$  is  $\lambda$  times the vector  $\overline{uv}$ , which yields

$$(q.x - u.x) = \lambda(v.x - u.x) \iff q.x = \lambda(v.x - u.x) + u.x \quad (10)$$

and

$$(q.y - u.y) = \lambda(v.y - u.y) \iff q.y = \lambda(v.y - u.y) + u.y, \quad (11)$$

whereas the latter implies

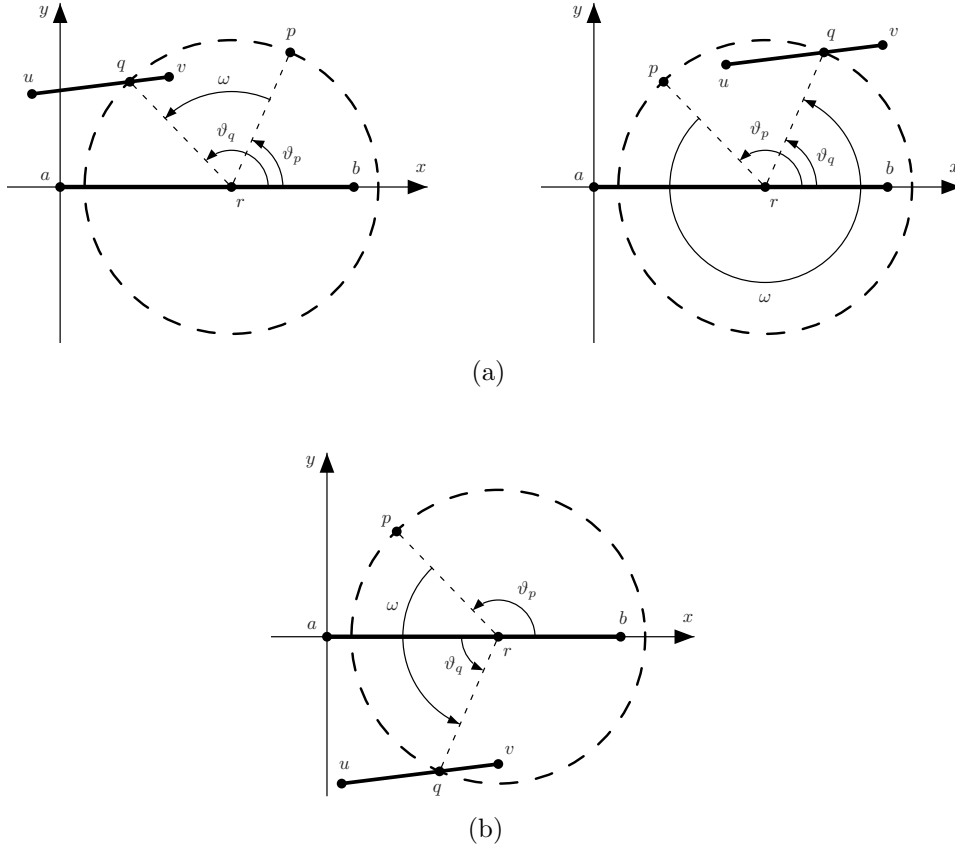


Figure 12: Parameterizing the intersection between the circle  $C_p(r)$  and the edge  $\overline{uv}$  while  $r$  moves along segment  $\overline{ab}$  when point  $p$  and the intersection  $q$  of  $C_p(r)$  and  $\overline{uv}$  are (a) in the same halfplane and (b) in opposite halfplanes (with respect to the  $x$ -axis).

$$\begin{aligned}
 d^2(q, r) &= d^2(p, r) \\
 \iff (q.x - x)^2 + (q.y)^2 &= (p.x - x)^2 + (p.y)^2 \\
 \iff (q.x)^2 - 2xq.x + (q.y)^2 - (p.x)^2 + 2xp.x - (p.y)^2 &= 0. \quad (12)
 \end{aligned}$$

By substituting  $q.x, q.y$  from equations 10 and 11 into Equation 12, we

get

$$\begin{aligned}
& [\lambda(v.x - u.x) + u.x]^2 - 2x[\lambda(v.x - u.x) + u.x] \\
& + [\lambda(v.y - u.y) + u.y]^2 - (p.x)^2 + 2xp.x - (p.y)^2 = 0 \\
\iff & \lambda^2 [(v.x - u.x)^2 + (v.y - u.y)^2] \\
& - 2\lambda [x(v.x - u.x) - u.x(v.x - u.x) - u.y(v.y - u.y)] \\
& - 2x(u.x - p.x) + (u.x)^2 + (u.y)^2 - (p.x)^2 - (p.y)^2 = 0,
\end{aligned}$$

which has at most 2 roots for  $\lambda$  in terms of  $x$  of the form

$$\lambda = \alpha(x) \pm \sqrt{\beta(x)}, \quad (13)$$

where  $\alpha(x)$  and  $\beta(x)$  are polynomials of degrees 1 and 2, respectively.

Then, by substituting  $q.x, q.y$ , and  $\lambda$  from equations 10, 11 and 13 respectively, into Equation 9, we get:

$$\cos(\omega) = \frac{\gamma(x) \pm \sqrt{\delta(x)}}{\epsilon(x)} \implies \omega = \arccos\left(\frac{\gamma(x) \pm \sqrt{\delta(x)}}{\epsilon(x)}\right), \quad (14)$$

where  $\gamma(x)$ ,  $\delta(x)$ , and  $\epsilon(x)$  are polynomials of degrees 2, 4, and 2, respectively.

## 4 3D Fixed MCR (Problem 3)

In this section we extend our techniques to the 3D-equivalent of Problem 1. We consider a set  $S$  of  $n$  points in 3D, a rotation center  $r$ , and a non self-intersecting polyhedron  $P$  with complexity  $m$ , i.e., with  $m$  facets. We identify rotations around  $r$  with points in a sphere with center  $r$ . The following shows how to extend the algorithm we used to solve the Fixed MCR problem:

1. **Compute the inclusion regions.** For each  $p_j \in S$ , the intersection of the sphere  $C_{p_j}(r)$  with center at  $r$  and radius  $|\overline{rp_j}|$  with the polyhedron  $P$  results in a set of regions on the boundary of the sphere. These regions consist of the rotated copies of  $p_j$  that lie in the interior of  $P$ .
  - Regardless of  $P$  being convex or not, each facet can contribute to those regions a constant number of times. Hence, the overall complexity is  $O(m)$ . Moreover, notice that a region can have many holes, even in the case that  $P$  is convex.
  - The sides of these regions on the sphere  $C_{p_j}(r)$  are arcs of circles, since they are the intersection of the sphere with a planar facet of the polyhedron. Then, these sides can be computed in constant time each, as the intersection of the planes containing the faces of the polyhedron with  $C_{p_j}(r)$ .

- Thus the total time and space complexities of computing all the  $O(nm)$  regions is  $O(nm)$ .
2. **Normalize inclusion regions.** Let  $R_{p_j}$  be the set of inclusion regions of  $p_j \in S$ . Consider the unit sphere  $S^2$  to be centered at  $r$  and project the regions to  $S^2$ . Choose a point  $N$  in  $S^2$  as reference and compute the rotation  $\tau_j$  required to send  $p_j$  to  $N$ . Then compute  $\tau_j(R_{p_j})$  to set the same reference for all the inclusion regions.
  3. **Computing the depth of  $N$ .** For later use, we need to compute how many of the above regions contain the point  $N$  (in its interior or boundary), what we call the *depth* of  $N$ . In order to compute it, we perform point location in the planar subdivision on the sphere, i.e., we check whether the point  $N$  belongs to each of the  $O(nm)$  regions with a cost of  $O(\log m)$  per region, for a total time complexity of  $O(nm \log m)$ .
  4. **Stereographic projection.** We use the well-known stereographic projection from the point  $N$ , considered as the north pole, to the tangent plane at the antipodal south pole. The fact that this projection is conformal implies that circles in the sphere are mapped to circles in the plane [9]. Therefore, the projections of the inclusion regions  $\tau_j(R_{p_j})$  have boundaries composed by circular arcs. Because any two sides (arcs of circles) of the regions can intersect at most two times, the arrangement  $\mathcal{A}$  of projected regions can be computed in  $O(n^2m^2)$  time and space, since the total number of intersection points between arcs is  $O(n^2m^2)$ . Notice that for computing the projected arc we proceed as follows: We compute the projection of the two endpoints of the arc, and also the projection of a third point of the arc (for example the corresponding to the midpoint of the arc); with these three projected points, we compute the circle containing the projected arc and the projected arc itself.
  5. **Computing the region in  $\mathcal{A}$  with largest depth.** To do this computation we work on the dual graph of the arrangement  $\mathcal{A}$ , just knowing that the exterior (unbounded) face of  $\mathcal{A}$  is the face which was containing the point  $N$ , and hence we know its depth. Starting in this face, we perform a traversal of the dual graph, computing the depth of each region and maintaining the region with maximum depth, in a total  $O(n^2m^2)$  time.

Computing an interior point of the region with maximum depth, we compute its corresponding point in the unit sphere and then we know the two parameters  $\theta, \varphi$  giving such direction, which is the solution of our problem.

**Theorem 13.** *The Fixed MCR problem in 3D can be solved in  $O(n^2m^2 \log(nm))$  time and  $O(n^2m^2)$  space.*

## 5 Concluding Remarks

We studied the problem of finding a rotation of a simple polygon that covers the maximum number of points from a given point set. We described algorithms to solve the problem when the rotation center is fixed, or lies on a line segment, a line, or a polygonal chain. Without much effort, our algorithms can also be applied when the polygon has holes, and can be easily modified to solve minimization versions of the same problems. We also solved the problem with a fixed rotation center in 3D, leaving as open problem the 3D-analogue of Problem 2.

## 6 Acknowledgements

David Orden is supported by MINECO Projects MTM2014-54207 and MTM2017-83750-P, as well as by H2020-MSCA-RISE project 734922 - CONNECT. Carlos Seara is supported by projects Gen. Cat. DGR 2017SGR1640, by MINECO MTM2015-63791-R, and by H2020-MSCA-RISE project 734922 - CONNECT. Jorge Urrutia is supported in part by SEP-CONACYT of México, Proyecto 80268 and by PAPIIT IN102117 Programa de Apoyo a la Investigación e Innovación Tecnológica, Universidad Nacional Autónoma de México..

## References

- [1] P. K. Agarwal, T. Hagerup, R. Ray, M. Sharir, M. Smid, and E. Welzl. Translating a planar object to maximize point containment. In *Algorithms — ESA 2002: 10th Annual European Symposium. Rome, Italy, September 17–21, 2002. Proceedings*, pages 42–53, 2002.
- [2] G. Barequet and A. Goryachev. Offset polygon and annulus placement problems. *Computational Geometry: Theory and Applications*, 47(3, Part A):407–434, 2014.
- [3] G. Barequet and S. Har-Peled. Polygon containment and translation min-hausdorff-distance between segment sets are 3SUM-hard. *International Journal of Computational Geometry & Applications*, 11(4): 465–474, 2001.
- [4] G. Barequet, M. Dickerson, and P. Pau. Translating a convex polygon to contain a maximum number of points. *Computational Geometry: Theory and Applications*, 8(4):167–179, 1997.



- [5] B. Chazelle. *Advances in Computing Research*, volume 1, chapter The polygon containment problem, pages 1–33. JAI Press, 1983.
- [6] M. Dickerson and D. Scharstein. Optimal placement of convex polygons to maximize point containment. *Computational Geometry: Theory and Applications*, 11(1):1–16, 1998.
- [7] A. Gajentaan and M. H. Overmars. On a class of  $O(n^2)$  problems in computational geometry. *Computational Geometry: Theory and Applications*, 5(3):165–185, 1995.
- [8] H. Ishiguro, M. Yamamoto, and S. Tsuji. Omni-directional stereo. *IEEE Transactions on Pattern Analysis and Machine Intelligence*, 14(2):257–262, 1992.
- [9] T. Needham. *Visual complex analysis*, chapter 6.II.3: A conformal map of the sphere, pages 283–286. Clarendon Press, Oxford, 1998.
- [10] C. K. Yap and E.-C. Chang. *Algorithms for Robot Motion Planning and Manipulation*, chapter Issues in the metrology of geometric tolerancing, pages 393–400. A.K. Peters, Wellesley, MA, 1997.